Supplementary Figure Legends

Supplementary Figure 1. Schema of our strategy to identify prognostic radiomic features. (A) The overlap of RFs screened by different methods. **(B)** Landscape of risk grouping of different RF prognostic models. **(C)** The relationship between the selected RFs by different methods and macrophage enrich score in LGG and GBM.

Supplementary Figure 2. The relationship between prognostic RFs and tumor cell functions in the external validation cohort. (A) The top 10 significant correlations between RFs and cell fractions in the external validation cohort. **(B)** The *pearson* correlation between RFs and macrophage cells signature in the external validation cohort. **(C)** The *pearson* correlation between RFs and endothelial cells signature in the external validation cohort.

Supplementary Figure 3. The cell composition of primary culture cells in patient PDC1. Single-cell transcriptional profiling identifies 7 discrete cell populations across immune cells and non-immune cells. Normalized expression of macrophage markers overlaid on tSNE plot. The gene includes PTPRC, ITGAM, CD14, FCGR3A, CD86, CD68, CD163.

Supplementary Figure 4. The cell composition of primary culture cells in patient PDC14. Single-cell transcriptional profiling identifies 5 discrete cell populations across immune cells and non-immune cells. Normalized expression of macrophage markers overlaid on tSNE plot. The gene include CD68, CD163, CD8A, CD3D, GZMA, PTPRC, ITGAM, CD14, FCGR3A, and CD86.

Supplementary Figure 5. The cell composition of primary culture cells in patient PDC7. Single-cell transcriptional profiling identifies 6 discrete cell populations across immune cells and non-immune cells. Normalized expression of macrophage markers overlaid on tSNE plot. The gene include CD68, CD163, CD8A, CD3D, GZMA, PTPRC, ITGAM, CD14, FCGR3A and CD86.

Supplementary Figure 6. The cell composition of primary culture cells in patient PDC12. Single-cell transcriptional profiling identifies 5 discrete cell populations across immune cells and non-immune cells. Normalized expression of macrophage markers overlaid on tSNE plot. The gene include PTPRC, ITGAM, CD14, FCGR3A, CD86, CD68, and CD163.

Supplementary Figure 7. Clinical outcome of immune related Macrophage cell signatures in patients with gliomas in high and low RF scores groups. (A-B) Kaplan –Meier survival analysis was performed between the samples with high and low macrophage cell enrichment scores. Compare the gene expression between low and high groups of RF scores. **(C-D)** In transcriptome sequencing data of gliomas in the discovery cohort, macrophage markers were enriched in high-risk samples and predicted poor prognosis.

Supplementary Figure 8. The *pearson* correlation between RFs and macrophage cells signature in LGG and GBM, respectively.

Supplementary Figure 9. IHC staining displayed the RF related macrophage markers of MS4A4A, STAB1 and COLEC12. The scatter diagram showed the expression level of these markers in high risk and low risk samples in LGG **(A, C and E)** and GBM **(B, D and F)**, respectively. Kaplan-Meier survival analysis was performed between the samples with high and low expression of macrophage markers in LGG **(A, C and E)** and GBM **(B, D and F)**, respectively.

Supplementary Figure 10. Verification of the prediction model based on deep learning algorithm (Deep learning model 1) in predicting the prognosis of glioma. (A) Work flow of the deep learning method (Deep learning Model 1). **(B)** *P*-value distribution representing -log10(*P*-value) (x-axis) and times(y-axis) for 300 times in cross validation. Kaplan-Meier curves showed the overall survival of in low risk and high risk patients grouping by deep learning method (Deep learning Model 1). Overall survival of patients in high risk group was significantly shorter in the discovery (Tiantan) **(C),** external validation (TCGA) **(E)** and prospective validation **(G)** cohorts. Univariate

and multivariate COX survival analysis of the predicted risk group and other prognostic factors in the discovery (Tiantan) **(D)**, external validation (TCGA) **(F)** and prospective validation **(H)** cohorts. The age is numerical variables and the risk group, WHO Grade, IDH Status, 1p/19q Codel Status and TCGA Subtype are categorical variables.

Supplementary Figure 11. Verification of the prediction model based on deep learning algorithm (Deep learning Model 2) in predicting the prognosis of glioma. **(A)** Work flow of the deep learning method (Deep learning Model 2). **(B)** *P*-value distribution representing -log10(*P*-value) (x-axis) and times(y-axis) for 300 times in cross validation. Kaplan-Meier curves showed the overall survival of in low risk and high risk patients grouping by deep learning method (Deep learning Model 2). Overall survival of patients in high risk group was significantly shorter in the discovery (Tiantan) **(C),** external validation (TCGA) **(E)** and prospective validation **(G)** cohorts. Univariate and multivariate COX survival analysis of the predicted risk group and other prognostic factors in the discovery (Tiantan) **(D)**, external validation (TCGA) **(F)** and prospective validation **(H)** cohorts. The age is numerical variables and the risk group, WHO Grade, IDH Status, 1p/19q Codel Status and TCGA Subtype are categorical variables.

Supplementary Figure 12. Verification of the prediction model based on deep learning algorithm (Deep learning Model 3) in predicting the prognosis of glioma. **(A)** Work flow of the deep learning method (Deep learning Model 3). **(B)** *P*-value distribution representing -log10(*P*-value) (x-axis) and times(y-axis) for 300 times in cross validation. Kaplan-Meier curves showed the overall survival of in low risk and high risk patients grouping by deep learning method (Deep learning Model 3). Overall survival of patients in high risk group was significantly shorter in the discovery (Tiantan) **(C),** external validation (TCGA) **(E)** and prospective validation **(G)** cohorts. Univariate and multivariate COX survival analysis of the predicted risk group and other prognostic factors in the discovery (Tiantan) **(D)**, external validation (TCGA) **(F)** and prospective validation **(H)** cohorts. The age is numerical variables and the risk group, WHO Grade, IDH Status, 1p/19q Codel Status and TCGA Subtype are categorical variables.

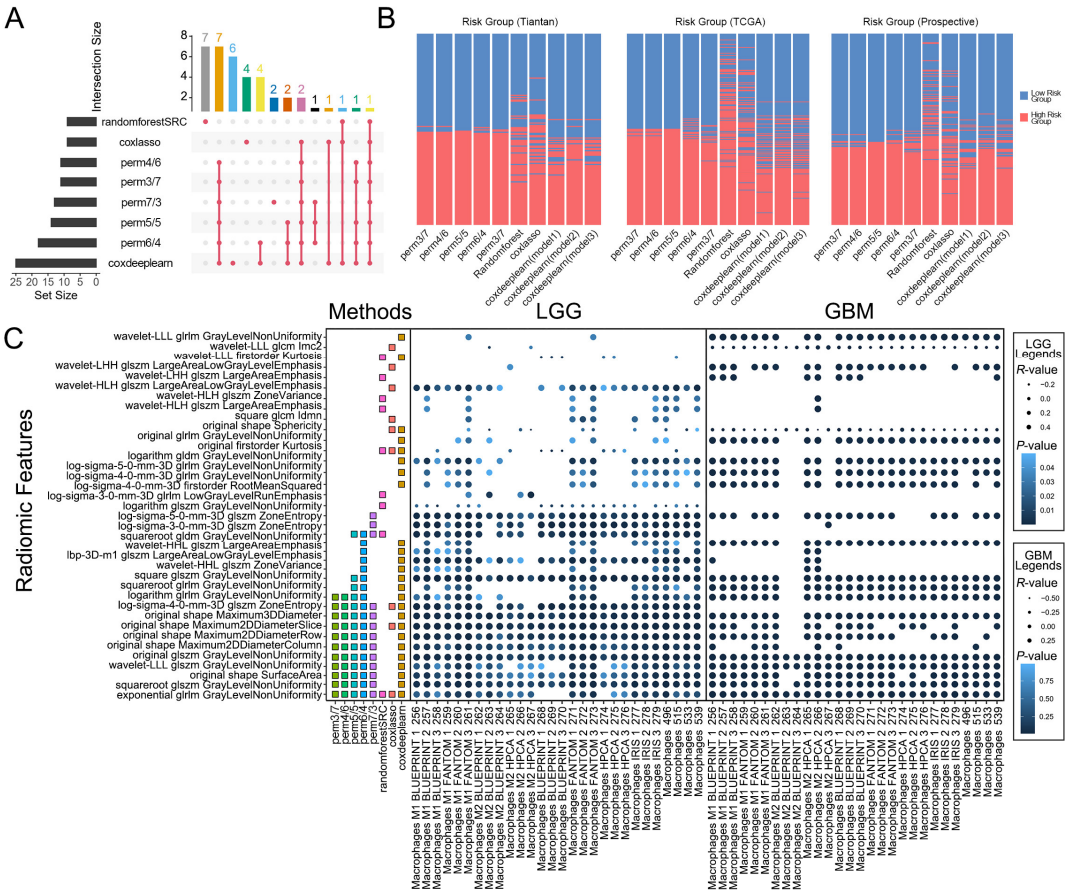

Supplementary Figure 1. Schema of our strategy to identify prognostic radiomic features.

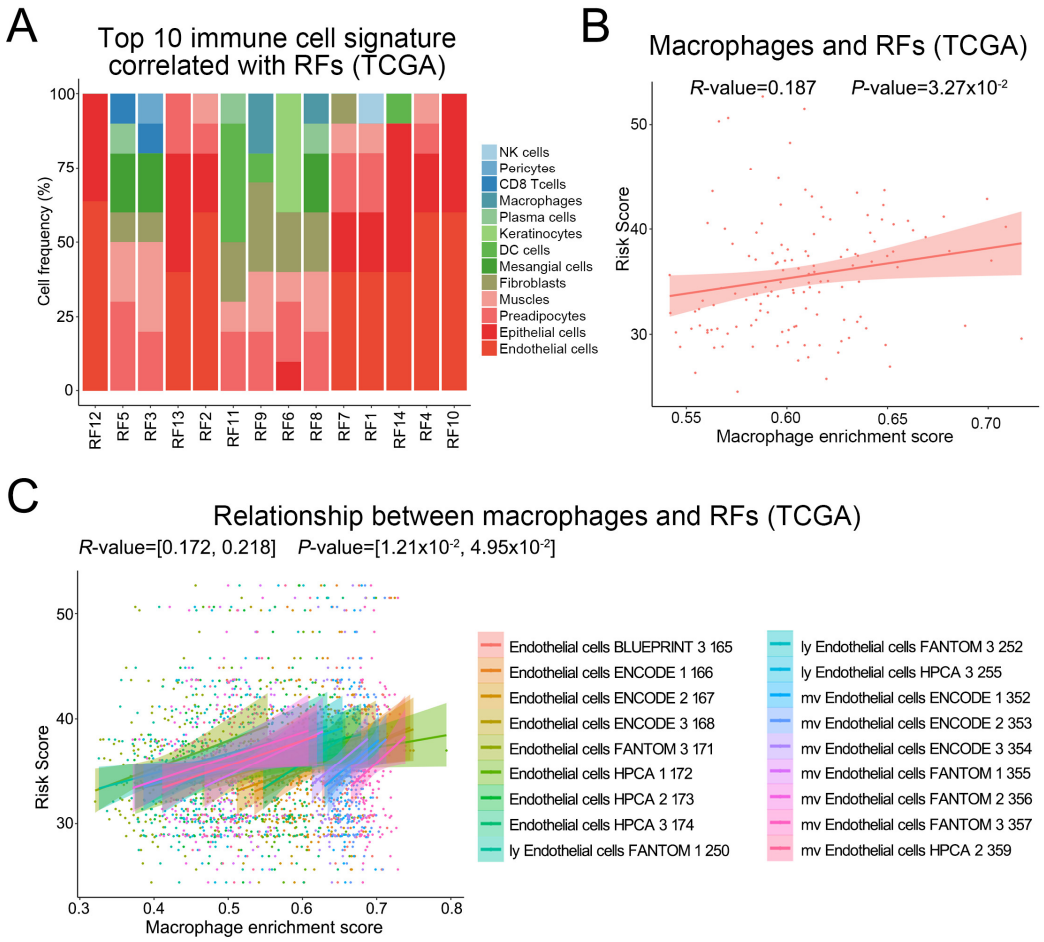

Supplementary Figure 2. The relationship between prognostic RFs and tumor cell functions in the external validation cohort.

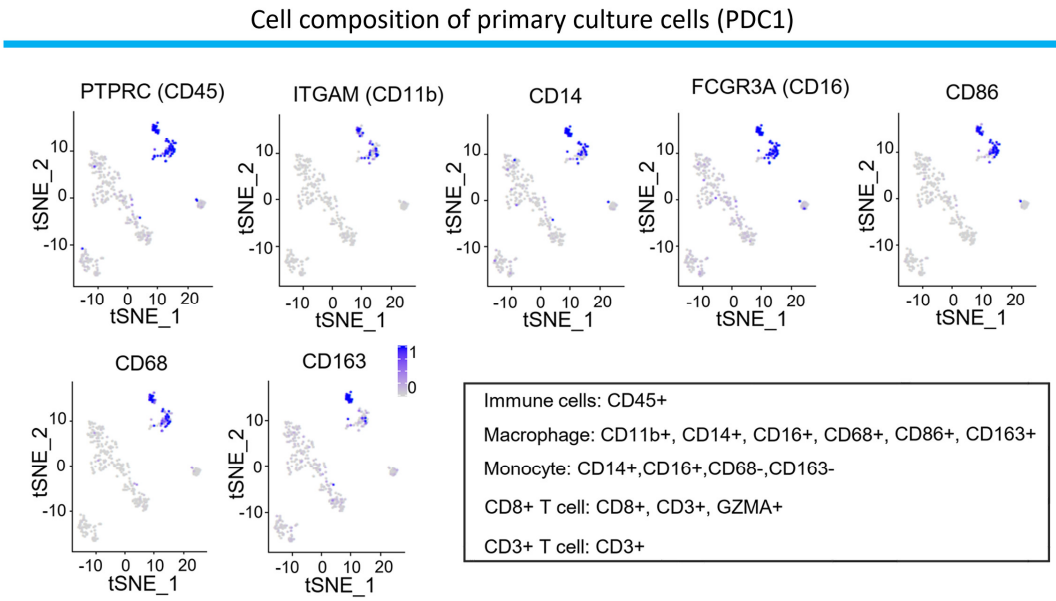

Supplementary Figure 3. The cell composition of primary culture cells in patient PDC1.

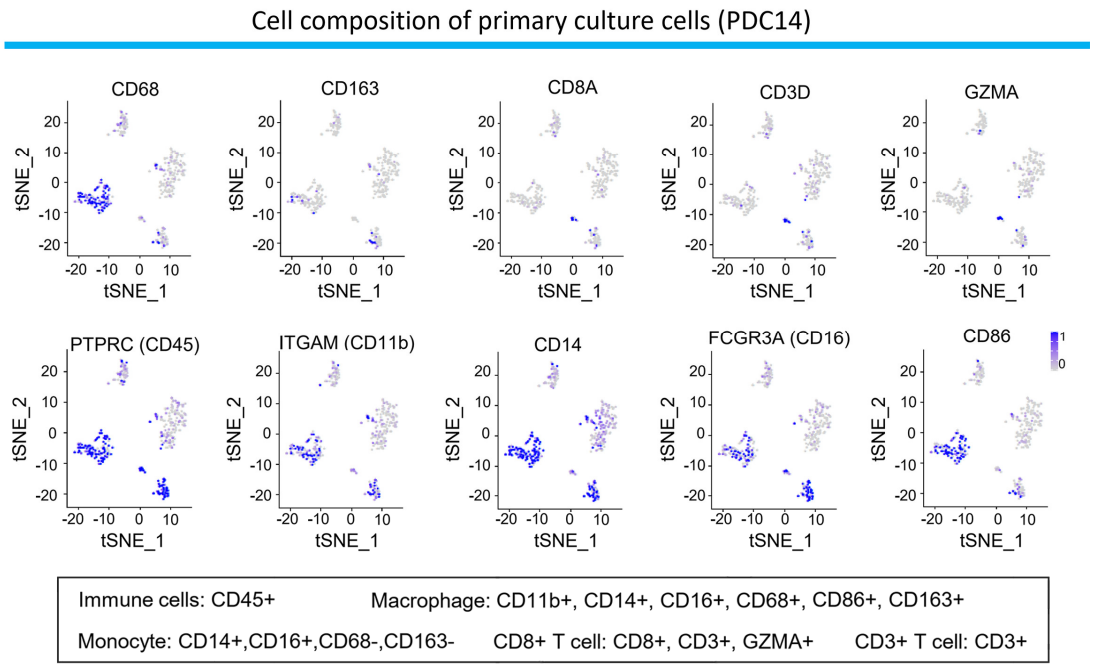

Supplementary Figure 4. The cell composition of primary culture cells in patient PDC14.

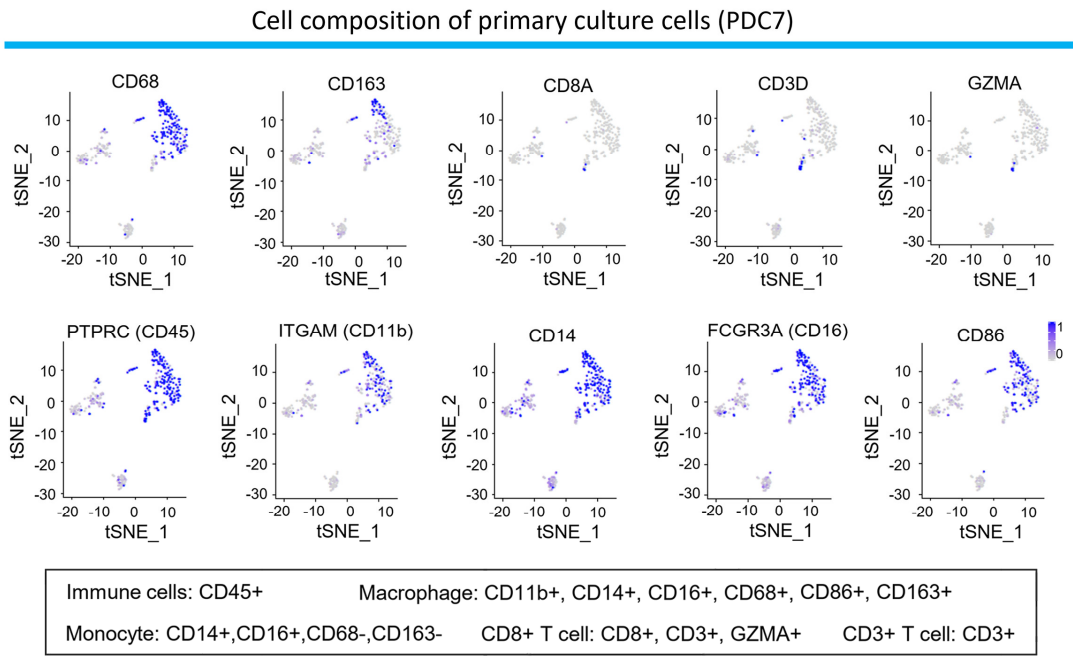

Supplementary Figure 5. The cell composition of primary culture cells in patient PDC7.

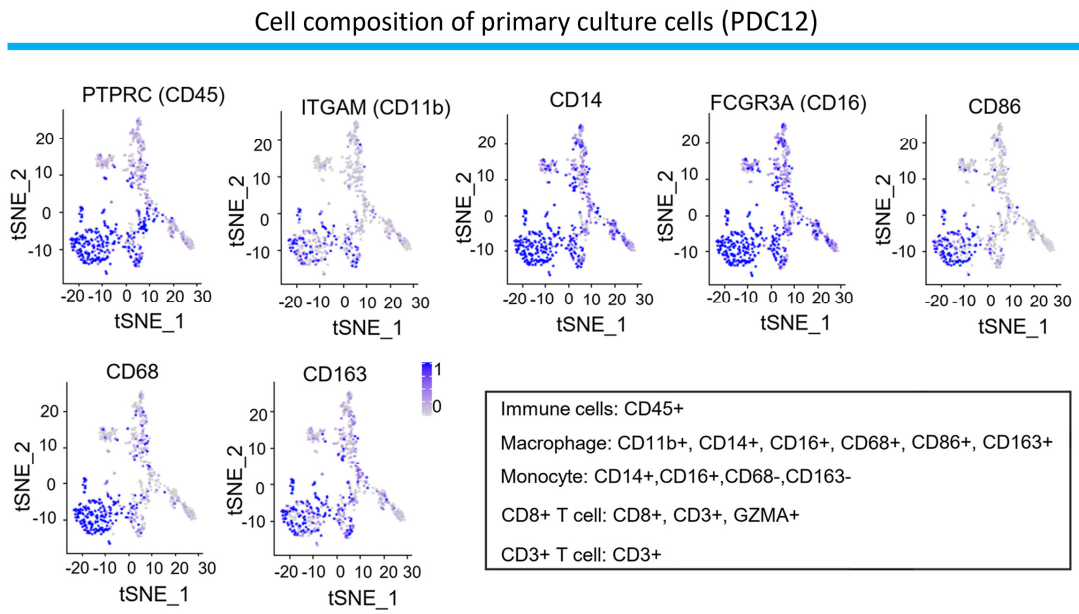

Supplementary Figure 6. The cell composition of primary culture cells in patient PDC12.

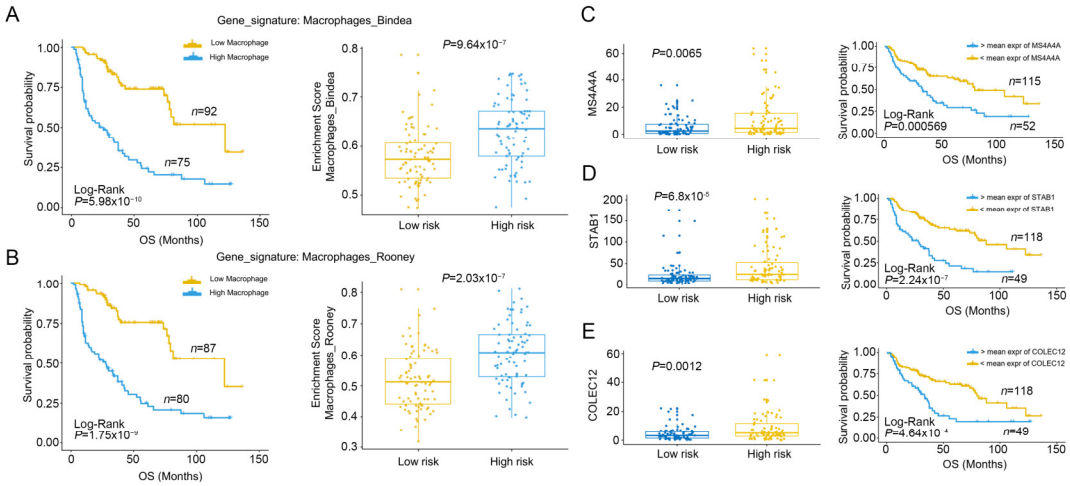

Supplementary Figure 7. Clinical outcome of immune related Macrophage cell signatures in patients with gliomas in high and low RF scores groups.

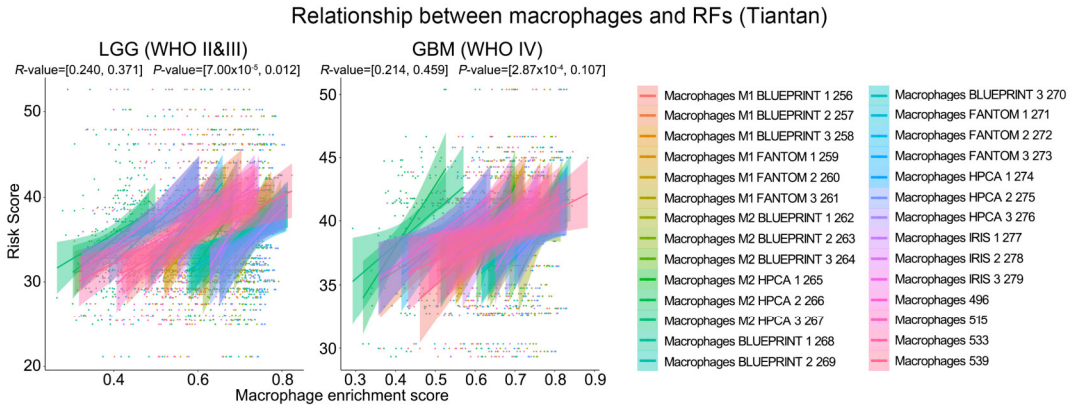

Supplementary Figure 8. The *pearson* correlation between RFs and macrophage cells signature in LGG and GBM, respectively.

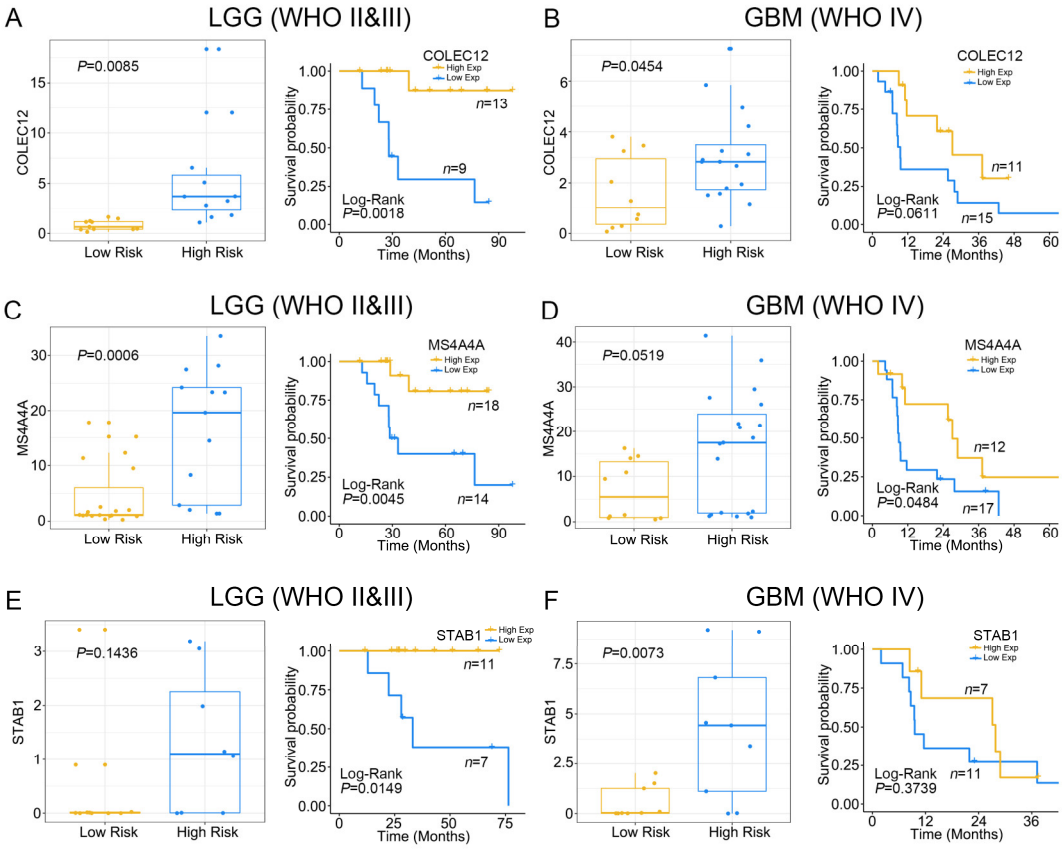

Supplementary Figure 9. IHC staining displayed the RF related macrophage markers of MS4A4A, STAB1 and COLEC12.

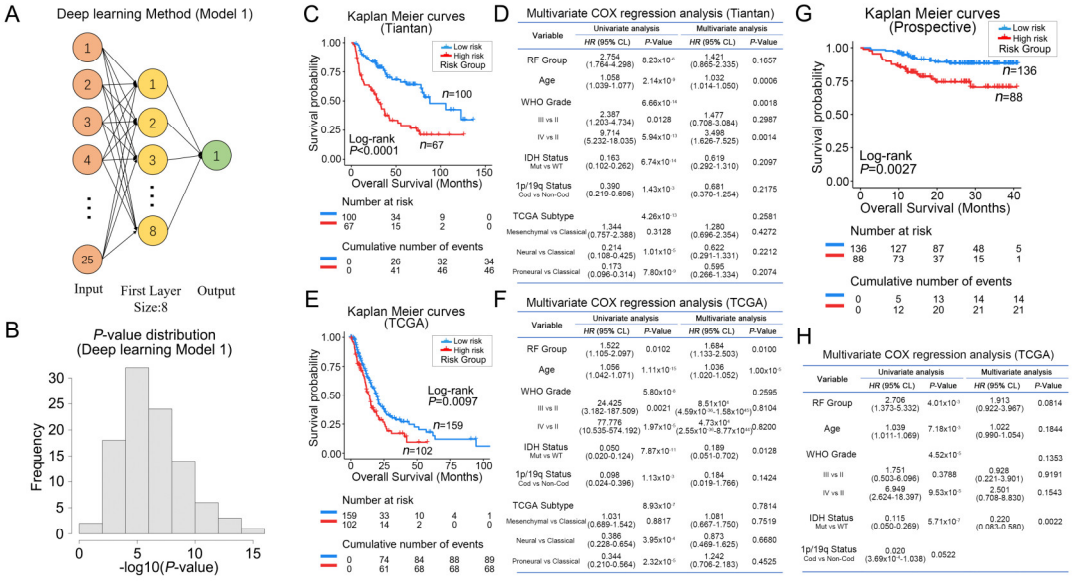

Supplementary Figure 10. Verification of the prediction model based on deep learning algorithm (Deep learning model 1) in predicting the prognosis of glioma.

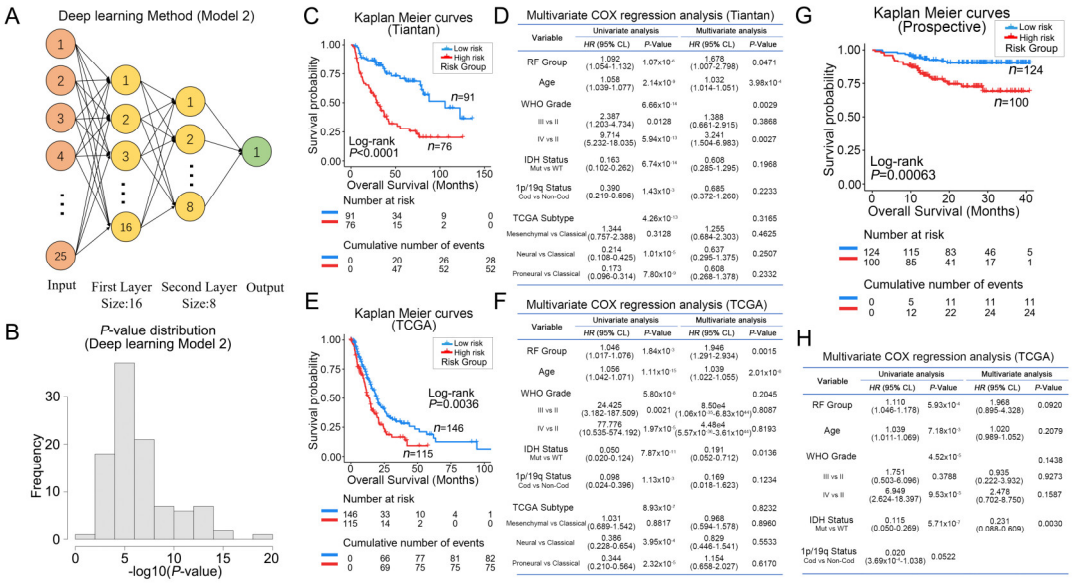

Variable	Univariate analysis		Multivariate analysis	
	HR (95% CL)	P-Value	HR (95% CL)	P-Value
RF Group	1.092 (1.054-1.132)	1.07×10^{-6}	1.676 (1.007-2.798)	0.0471
Age	1.058 (1.039-1.077)	2.14×10^{-9}	1.032 (1.014-1.051)	3.98×10^{-4}
WHO Grade		6.66×10^{-14}		0.0029
III vs II	2.387 (1.203-4.734)	0.0128	1.388 (0.661-2.915)	0.3868
IV vs II	9.714 (5.232-18.035)	5.94×10^{-13}	3.241 (1.504-6.983)	0.0027
IDH Status Mut vs WT	0.163 (0.102-0.262)	6.74×10^{-14}	0.608 (0.285-1.295)	0.1968
1p/19q Status Cod vs Non-Cod	0.390 (0.210-0.696)	1.43×10^{-3}	0.685 (0.372-1.260)	0.2233
TCGA Subtype		4.26×10^{-13}		0.3165
Mesenchymal vs Classical	1.344 (0.757-2.388)	0.3128	1.255 (0.684-2.303)	0.4625
Neural vs Classical	0.214 (0.108-0.425)	1.01×10^{-5}	0.637 (0.295-1.375)	0.2507
Proneural vs Classical	0.173 (0.096-0.314)	7.80×10^{-9}	0.608 (0.268-1.378)	0.2332

Variable	Univariate analysis		Multivariate analysis	
	HR (95% CL)	P-Value	HR (95% CL)	P-Value
RF Group	1.046 (1.017-1.076)	1.84×10^{-3}	1.946 (1.291-2.934)	0.0015
Age	1.056 (1.042-1.071)	1.11×10^{-15}	1.039 (1.022-1.055)	2.01×10^{-6}
WHO Grade		5.80×10^{-6}		0.2045
III vs II	24.425 (3.182-187.509)	0.0021	8.50e4 (1.06×10^{-23}-$6.83\times10^{+44}$)	0.8087
IV vs II	77.776 (10.535-574.192)	1.97×10^{-5}	4.48e4 (5.57×10^{-18}-$3.61\times10^{+41}$)	0.8193
IDH Status Mut vs WT	0.050 (0.020-0.124)	7.87×10^{-11}	0.191 (0.052-0.712)	0.0136
1p/19q Status Cod vs Non-Cod	0.098 (0.024-0.396)	1.13×10^{-3}	0.169 (0.018-1.623)	0.1234
TCGA Subtype		8.93×10^{-7}		0.8232
Mesenchymal vs Classical	1.031 (0.689-1.542)	0.8817	0.968 (0.594-1.578)	0.8960
Neural vs Classical	0.386 (0.228-0.654)	3.95×10^{-4}	0.829 (0.446-1.541)	0.5533
Proneural vs Classical	0.344 (0.210-0.564)	2.32×10^{-5}	1.154 (0.658-2.027)	0.6170

Variable	Univariate analysis		Multivariate analysis	
	HR (95% CL)	P-Value	HR (95% CL)	P-Value
RF Group	1.110 (1.046-1.178)	5.93×10^{-4}	1.968 (0.895-4.328)	0.0920
Age	1.039 (1.011-1.069)	7.18×10^{-3}	1.020 (0.989-1.052)	0.2079
WHO Grade		4.52×10^{-5}		0.1438
III vs II	1.751 (0.503-6.096)	0.3788	0.935 (0.222-3.932)	0.9273
IV vs II	6.949 (2.624-18.397)	9.53×10^{-5}	2.478 (0.702-8.750)	0.1587
IDH Status Mut vs WT	0.115 (0.050-0.269)	5.71×10^{-7}	0.231 (0.088-0.609)	0.0030
1p/19q Status Cod vs Non-Cod	0.020 (3.69×10^{-4}-1.038)	0.0522		

Supplementary Figure 11. Verification of the prediction model based on deep learning algorithm (Deep learning Model 2) in predicting the prognosis of glioma.

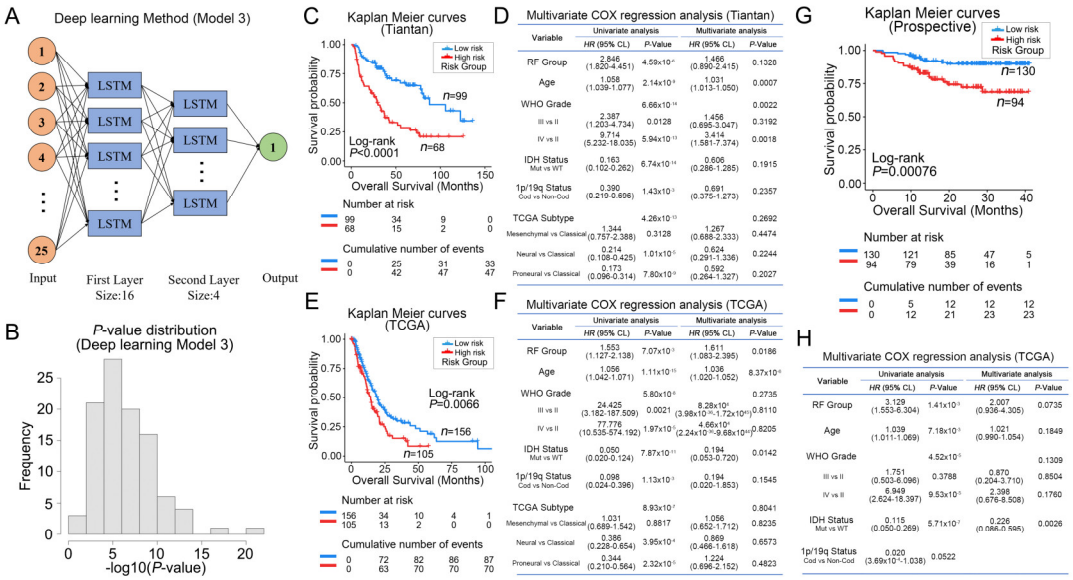

Supplementary Figure 12. Verification of the prediction model based on deep learning algorithm (Deep learning Model 3) in predicting the prognosis of glioma.

Supplementary Table 1 Characteristics of Patients in three independent cohorts

Characteristic	Discovery cohort (Tiantan)	External Validation Cohort (TCGA)	Prospective Validation Cohort (Beijing Tiantan Hospital)	*P*-value
Age (years)				<0.0001[a]
Mean	44.08	54.08	45.60	
SD	12.20	16.23	13.1	
Gender (No.)				0.0339[b]
Male	107	141	115	
Female	60	120	109	
WHO Grade (No.)				<0.0001[b]
II	65	49	77	
III	44	45	61	
IV	58	167	86	
IDH1 Status (No.)				<0.0001[b]
Mutation	100	75	129	
Wildtype	67	157	70	
Not Available	0	29	25	
1p/19q Status (No.)				<0.0001[b]
Co-deletion	54	22	62	
Non Co-deletion	112	231	98	
Not Available	1	8	64	

[a]Kruskal-Wallis test
[b]Chi-square test

Supplementary Table 2 Characteristics of Patients in the Discovery Cohort (Tiantan)

Characteristic	Low Risk	High Risk	*P*-value
Age (years)			0.1319[a]
Mean	42.77	45.41	
SD	10.86	13.43	
Gender (No.)			0.2178[b]
Male	50	57	
Female	34	26	
WHO Grade (No.)			<0.0001[b]
II	47	18	
III	21	23	
IV	16	42	
IDH1 Status (No.)			0.015[b]
Mutation	58	42	
Wildtype	26	41	
1p/19q Status (No.)			0.1214[b]
Co-deletion	32	22	
Non Co-deletion	52	60	
Not Available	0	1	

[a]Mann Whitney test
[b]Chi-square test

Supplementary Table 3 Characteristics of Patients in the External Validation Cohort (TCGA)

Characteristic	Low Risk	High Risk	*P*-value
Age (years)			0.0645[a]
Mean	52.18	55.93	
SD	16.05	16.24	
Gender (No.)			0.0561[b]
Male	62	79	
Female	67	53	
WHO Grade (No.)			0.0001[b]
II	36	13	
III	26	19	
IV	67	100	
IDH1 Status (No.)			0.0166[b]
Mutation	47	28	
Wildtype	72	85	
Not Available	10	19	
1p/19q Status (No.)			0.1744[b]
Co-deletion	14	8	
Non Co-deletion	112	119	
Not Available	3	5	

[a]Mann Whitney test
[b]Chi-square test

Supplementary Table 4 Characteristics of Patients in the Prospective Validation Cohort (Beijing Tiantan Hospital)

Characteristic	Low Risk	High Risk	*P*-value
Age (years)			0.0006[a]
Mean	42.73	49.29	
SD	13.47	11.68	
Gender (No.)			0.0715[b]
Male	58	57	
Female	68	41	
WHO Grade (No.)			<0.0001[b]
II	60	17	
III	33	28	
IV	33	53	
IDH1 Status (No.)			0.008[b]
Mutation	84	45	
Wildtype	32	38	
Not Available	10	15	
1p/19q Status (No.)			0.1925[b]
Co-deletion	40	22	
Non Co-deletion	53	45	
Not Available	33	31	

[a]Mann Whitney test
[b]Chi-square test